Coulombic force contribution to nano scale aerosol capture by a wire grid: Quantitative comparison of experiments and simulations

Siddharth Rajupet, Soleiman Bourrous, Francois Gensdarmes, Mamadou Sow

Coulombic force contribution to nano scale aerosol capture by a wire grid: Quantitative comparison of experiments and simulations

Siddharth Rajupet[a,b], Soleiman Bourrous[b], Francois Gensdarmes[b], Mamadou Sow[b*]
[a]*Department of Chemical and Biomolecular Engineering, Case Western Reserve University, Cleveland, OH, USA*
[b]*Institut de Radioprotection et de Sûreté Nucléaire (IRSN), PSN-RES, SCA, Gif-sur-Yvette, 91192, France*
[*]mamadou.sow@irsn.fr

Abstract:

Fibers of filter media and aerosol particles both typically have some distributions of electric charge. Attractive coulombic interactions between charged particles and fibers enhance aerosol filtration efficiency; however, these coulombic interactions are difficult to characterize due to the complex, nonuniform fiber charge, diameter and spacing of typical filter media. We develop an experimental filter assembly to control these coulombic interactions. The filter assembly consists of three sequential electrically isolated metallic grids—high voltage is applied to the middle grid and the adjacent outer grids are electrically grounded such that the electric potential distribution in the filter assembly is well-defined. We test this filter assembly with aerosols of controlled diameter (ranging between ~70 - 500 nm) and electric charge ($1e^-$), and systematically increase the applied voltage to the middle grid to enhance coulombic interactions and consequently the filter efficiency. We develop particle trajectory simulations to model our experimental filter assembly such that all parameters in the simulation have direct basis from the experimental system. We find excellent quantitative agreement between the filter efficiency measured in experiments and predicted from simulations *without any fitting parameters*. The precise control and accurate simulation of coulombic interactions demonstrated in this study indicate that the experimental and simulation methodologies developed here may be applied to uncover fundamental insights into the role of coulombic forces in more complex phenomena such as filter clogging.

I. INTRODUCTION

The filtration of aerosols is of significant interest in a number of environmental, health, and safety applications including mitigating indoor and outdoor air pollution (Vohra et al., 2021), reducing the transmission of respiratory viruses (Anderson, Turnham, Griffin, & Clarke, 2020; Cowling et al., 2013), and preventing dissemination of airborne hazardous materials (Kaneyasu, Ohashi, Suzuki, Okuda, & Ikemori, 2012; Malá, Rulík, Bečková, Mihalík, & Slezáková, 2013; Povinec et al., 2012). We are particularly interested in the filtration of radioactive aerosols, which may be produced from fires, liquid leaks, or general dismantling processes of nuclear plants and laboratories (Halverson, Ballinger, & Dennis, 1987; Sow et al., 2020; Sow, Leblois, & Gensdarmes, 2019).The efficiency of filters at capturing aerosols depends on the aerosol size and typically, filters are least effective at capturing aerosols with diameters between ~100-300 nm—this size range is termed the maximum penetrating particle size (MPPS). Aerosol particles within this size range are particularly hazardous to health since they penetrate deep into human respiratory pathways and disseminate far from their source.

Aerosols and fibers of filters typically have a distribution of charge, and attractive electrostatic interactions between particles and fibers are well-known to increase filtration efficiency, particularly within the MPPS range (Alonso, Alguacil, Santos, Jidenko, & Borra, 2007; Kerner et al., 2020; Thakur, Das, & Das, 2013; D. C. Walsh & Stenhouse, 1997a, 1997b, 1998; D. Walsh & Stenhouse, 1996; M. Zhao et al., 2020) where other aerosol capture mechanisms like diffusion and impaction are less effective. These interactions include coulombic interactions, where charged fibers attract charged particles, dielectrophoric interactions, where charged fibers polarize particles, and image forces, where charged particles polarize fibers. Improving filter efficiency by incorporating electrostatic interactions is particularly advantageous since the efficiency is improved without increasing the pressure drop of the filter. As a result, the fabrication of filters typically includes steps to impart electrostatic charge and several recent studies have sought to enhance electrostatic interactions by applying external electric fields during filtration to directly charge, or polarize fibrous filter media (Choi et al., 2018, 2017; K. S. Han et al., 2019; S. Han, Kim, & Ko, 2021; Jeong et al., 2017; Tian & Mo, 2019; Tian et al., 2021; G. H. Zhang et al., 2020; R. Y. Zhang & Hsieh, 2020; K. Zhao et al., 2020).

The role of electrostatic effects on the efficiency of a clean filter has been evaluated theoretically by analytically determining the trajectories of particles around a single fiber while accounting for electrostatic forces (Kraemer & Johnstone, 1956; Natanson, 1957; Zebel, 1965). However, rigorous quantitative comparison of the electrostatic filtration efficiency between theory and experiments has never been achieved due to the complex structure of industrially manufactured filters. Traditional non-woven filters have a distribution of fiber diameters and inter-fiber spacings. Furthermore, experimentally characterizing the charge on fibers of filters through direct methods is challenging—this charge is non-uniform with different fibers having different polarities of charge (Kilic, Shim, & Pourdeyhimi, 2015; Thakur, Das, Das, & Reddy, 2015). Instead, a more common method to estimate the charge on fibers is to measure the initial efficiency of a filter and *fit* the fiber charge based on analytic theory (Baumgartner & Loffler, 1986; Kim, Otani, Noto, Namiki, & Kimura, 2005; Lathrache & Fissan, 1986; Lathrachi, Fissan, & Neuman, 1986; Lee,

Otani, Namiki, & Emi, 2002; Romay, Liu, & Chae, 1998; Thomas, Mouret, Cadavid-Rodriguez, Chazelet, & Bémer, 2013; D. C. Walsh & Stenhouse, 1997a, 1997b, 1998; D. Walsh & Stenhouse, 1996; Wu, Colbeck, & Zhang, 1993) or particle trajectory simulations (Kerner et al., 2018, 2020). This method, however, precludes the rigorous experimental validation of theory describing electrostatic effects in filtration.

A method to circumvent the difficulty in characterizing filter charge is to directly apply a potential to a conductive filter. In prior studies, traditional nonwoven filters were coated with aluminum and the filtration efficiency was enhanced by increasing the voltage applied to the filter (Choi et al., 2018, 2017). However, even when the potential of the fibers is controlled, the electric field distribution (and consequently the coulombic forces acting on the particles) near the filter is difficult to characterize due to non-uniformity in fiber size, orientation, and spacing in the filter—these factors strongly influence the electric field distribution when constant potential is applied. Such complexities make it difficult to quantitatively predict the contribution of electrostatic mechanisms to the global efficiencies of real fibrous filters using simulations.

Here we develop novel experimental and simulation methodologies through which we can quantitatively—and non-empirically—compare electrostatic filtration efficiencies in experiments and fundamental particle trajectory simulations, enabling rigorous understanding of the basis of electrostatic mechanisms on filtration performance. In our experiments, we carefully control the properties of both the aerosol particles and the filter media. To control the filter properties, we use a metallic grid with uniform fiber diameter and spacing as the filter and we control the fiber charge by applying a potential to this metallic grid such that the electric field distribution in our system is always well-defined. We then develop particle trajectory simulations based on the fundamental forces acting on particles as they flow past an individual fiber representative of a fiber in the high-voltage metallic grid. All parameters in our simulation have a direct basis from our experimental system i.e. *no fitting parameters are used*. Finally, we compare the electrostatic filtration efficiency measured in our experimental bench to that determined from the simulations.

II. METHODS

A. Experiments

To rigorously investigate the effect of electrostatic forces in aerosol filtration, we develop an experimental system in which we control the size and charge of aerosol particles as well as the size, spacing, and charge of fibers in our filter media. We then evaluate how the aerosol penetration through the filter (i.e. the fraction of aerosols passing through and not captured by the filter) varies with the electrostatic properties of the aerosol particles and filter.

We generate a monodisperse aerosol stream with a controlled charge, by first aerosolizing a solution of monodisperse polystyrene latex (PSL) particles (unless otherwise specified) using a constant output collision type atomizer (TSI Model 3076). After generation, the aerosol droplets pass through a diffusion dryer to evaporate the liquid to form a dry aerosol. The dried aerosol stream has a stable number concentration and size distribution. Then, we use a differential mobility

analyzer (DMA) (TSI Electrostatic Classifier Model 3082) to select only the monodisperse PSL particles carrying one elementary charge in the aerosol stream by precipitating other particles based on their electrical mobility. Only particles within a narrow range of electrical mobilities pass through the DMA such that the particles exiting the DMA are monodisperse and are charged with $1e^-$ (the particles have negative polarity). Due to the narrow size distribution of particles generated in our system and the relatively small particle sizes considered in this study, the fraction of particles exiting the DMA with multiple elementary charges is negligible. The schematic of the experimental system is depicted in Fig. 1.

We develop a filter with well-characterized geometry and electrostatic potential, as depicted in Fig. 2. The filter assembly consists of three identical metallic grids in series, which are electrically insulated from each other using polyether ether ketone (PEEK) spacers. The fibers of the metallic grids have a diameter of D_f = 100 µm and edge-to-edge spacing of h = 250 µm. The PEEK spacers are annuli with inner diameter of 35 mm, outer diameter of 47 mm and thickness of 11 mm such that the metallic grids are separated from each other by d = 11 mm and the filter cross sectional diameter exposed to the aerosol stream is 35 mm. The middle grid is connected to a positive high-voltage supply and the outer two grids are connected to electrical ground such that the electric potential in the filter assembly has well-defined boundaries. The electric field within the assembly is oriented such that particles are attracted to fibers of the center grid both when particles are upstream and downstream of the center grid. The filter assembly is placed inside a standard conical metallic 47 mm filter holder which is connected to electrical ground.

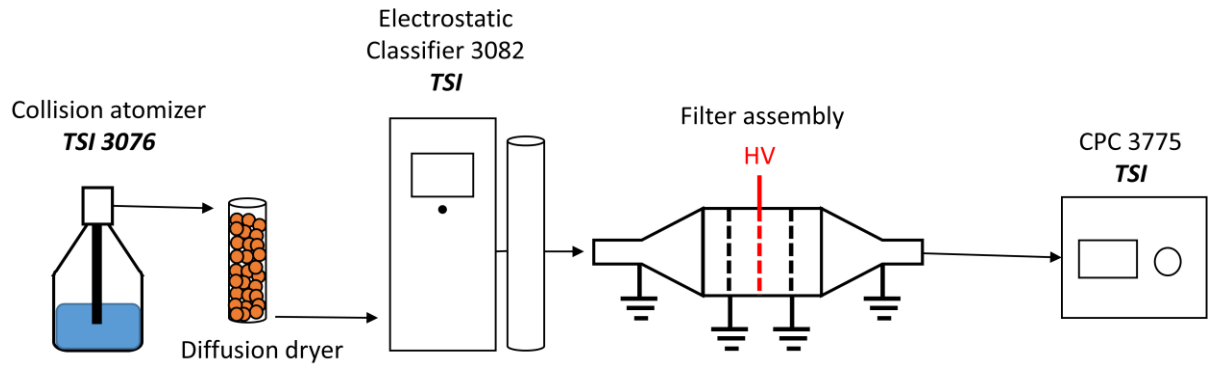

Figure 1. Schematic of experimental system. At the outlet of the Electrostatic Classifier 3082, the aerosol is composed of monodisperse, singly charged PSL particles. The electric potential of the metallic grid is controlled using a high-voltage supply.

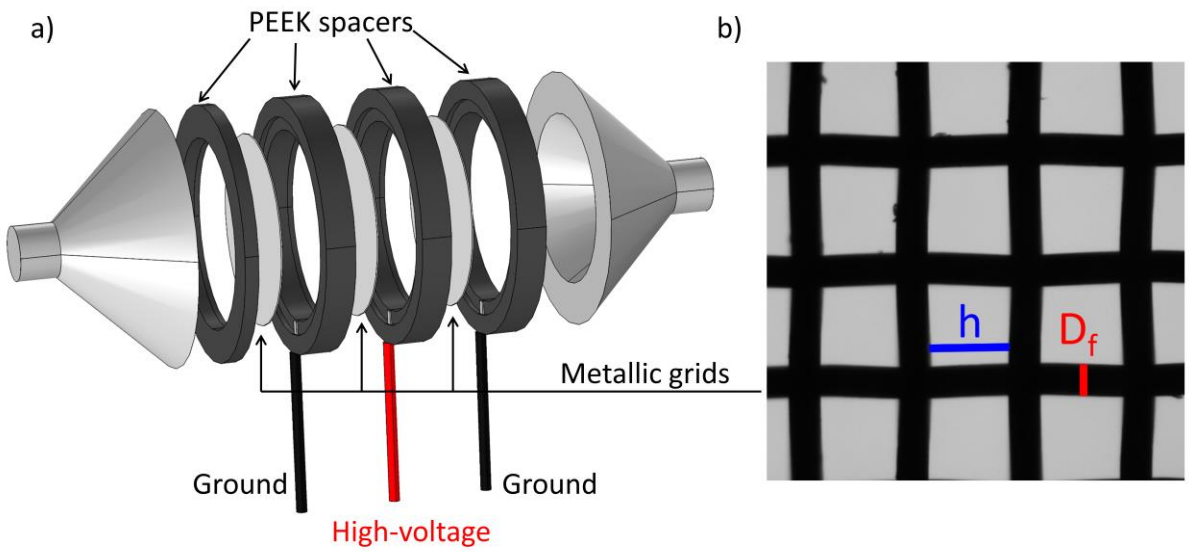

Figure 2. a) Schematic of filter assembly. The three metallic grids are insulated from each other and the conical filter holder by PEEK spacers. The middle grid contacts a positive high-voltage line while the outer two grids are connected to electrical ground. The thickness of the PEEK spacers is d = 11 mm such that the metallic grids are separated by 11 mm. b) Optical microscope images of the metallic grid used as the filter media. The edge-to-edge distance between fibers is h = 250 µm and the fiber diameter is D_f = 100 µm.

The monodisperse, singly charged aerosol flows through the filter assembly and the aerosol concentration after the filter assembly is measured by a Condensation Particle Counter (CPC) (TSI Model 3775). The average airflow face velocities examined ranged between 0.6 – 5 cm/s and in our analysis was considered to be uniform over the face of the grids. Thus, we do not account for nonuniform inlet fluid velocities which may arise in experiments due to undeveloped flow profiles or edge effects at the perimeter of the filter holder. However, due to the small fluid velocities tested (<5 cm/s) we do not expect these effects to be significant. We measure the aerosol concentration when no voltage difference is applied between the center and outer grids of the filter assembly, $C_{V=0}$. Then, we apply a voltage difference between the center and outer grids of the filter assembly and measure the aerosol concentration, $C_{V>0}$.

We test experimental conditions which help isolate coulombic effects. In particular, we choose particle sizes within the MPPS regime (~70 – 500 nm) and large fiber diameters (100 µm) such that mechanical capture mechanisms, i.e., diffusion, interception, and inertia, are less significant and the primary contributor to the aerosol capture efficiency is attractive coulombic forces between the negatively charged particles and positively charged metallic grid. To further distinguish the role of electrostatic forces from mechanical capture, we assume mechanical and coulombic mechanisms of particle capture are entirely independent (i.e. $C_{V=0} = P_{mech}^{exp} C_o$ and $C_{V>0} = P_{mech}^{exp} P_{coul}^{exp} C_o$ where C_o is the constant aerosol concentration upstream the grid, and P_{mech}^{exp} and P_{coul}^{exp}

are the penetration of particles through the metallic grids due to mechanical and coulombic interactions respectively). If P_{mech}^{exp} is the same with and without voltage applied, the ratio $P_{coul}^{exp} = C_{V>0}/C_{V=0}$ represents the penetration of particles through the metallic grids only due to coulombic interactions. The physical interpretation of P_{coul}^{exp} assumes that mechanical and coulombic mechanisms of particle capture are independent; however, given the little prevalence of mechanical capture in our system, we expect error due to this assumption to be insignificant.

B. Simulation

We simulate the trajectories of particles based on the fundamental forces acting on the particles as they flow past a single fiber and relate the fraction of particles captured by the fiber in our simulation to the total aerosol penetration through a full metallic grid. Our simulation cell is characteristic of a fiber within the center, high-voltage, grid of our experimental filter assembly. A circular fiber of diameter D_f = 100 µm is positioned in the center of a rectangular simulation cell depicted in Fig. 3. The width of the simulation cell is $2d$ = 22 mm and the height of the simulation cell is $D_f + h$ = 350 µm. The simulation is carried out in two dimensions such that the simulation represents particles flowing around infinitely long cylindrical fibers oriented parallel to each other.

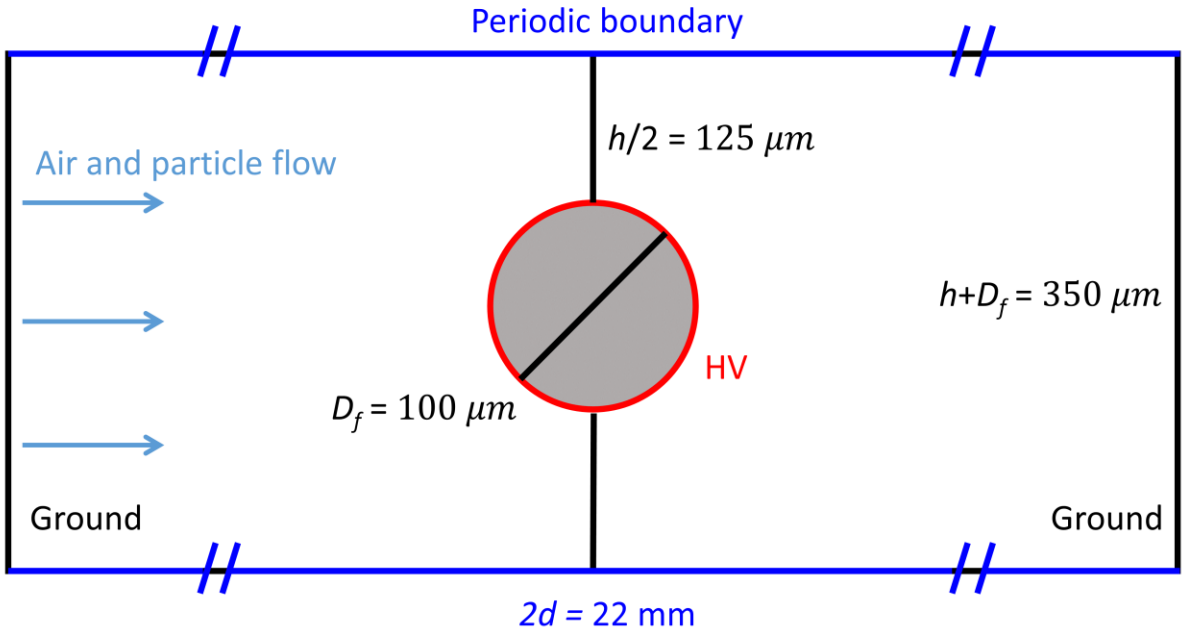

Figure 3. Schematic of simulation cell. The simulation cell is characteristic of a single fiber within the middle, high-voltage metallic grid and all parameters are taken directly from the experimental system i.e *no fitting parameters are used.*

In simulating the particle trajectories, we consider forces due to the airflow as well as coulombic forces between the particle and fiber. First, we solve the Navier-Stokes equations to determine the laminar fluid flow field and Poisson's equation to determine electrostatic potential field in the

system. We model the particles as spheres with diameter D_p with a single elementary charge. The forces due to airflow are then calculated using Stokes law together with the fluid flow field, and the coulombic forces are calculated from the gradient of the electrostatic potential field. We assume the particles have no effect on the fluid flow and potential field and the fluid velocity and electric field at the center of the particle are used to calculate the drag force and coulombic force respectively. Note, random fluctuations in particle position due to Brownian motion are not considered in the simulation.

The Navier-Stokes equations are solved using finite element methods. The fluid is modeled using properties of air and enters through the left boundary of the simulation cell with a uniform velocity profile u. The surface of the fiber has a no-slip boundary condition and the top and bottom of the rectangular cell have periodic boundary conditions.

Poisson's equation is also solved using finite element methods. We model the fiber with a constant surface potential ΔV and the left and right boundaries of the simulation with $V = 0$, characteristic of the two grounded metallic grids in our filter assembly. The top and bottom of the rectangular cell have periodic boundary conditions and the cell is modeled with dielectric properties characteristic of air. We emphasize that unlike the potential distribution in the constant charged fiber case, the potential distribution in the present system (with constant potential fibers) does not have an analytic solution preventing the use of more classical single fiber theory (Natanson, 1957).

We simulate the particle trajectories by integrating Newton's law of motion. We simulate the trajectories of n_o particles, with n_o = 10,000. The initial positions of the particles are evenly distributed on the left boundary of the simulation cell and with initial velocities equal to the airflow velocity, u. As the particles move, if the boundary of the particle contacts the fiber surface, the particle is considered captured by the fiber; the number of particles captured is denoted n_c. The fraction of particles collected, n_c/n_o, can be compared with the fraction of cross-sectional area that is blocked by the fiber, $D_f/(D_f+h)$, to give the collection efficiency of the single fiber due to coulombic interactions, η_C,

$$\eta_C = \frac{n_c}{n_o}\left(\frac{D_f+h}{D_f}\right) \tag{1}$$

Physically, all particles with initial positions within $\eta_C(D_f+D_p)/2$ of the center of a fiber are captured. From η_C in the simulation, we can estimate a total coulombic penetration by considering fibers arranged in a grid pattern as shown in Fig. 4, similar to that in the experiments. We assume η_C, which is calculated for fibers oriented parallel to each other, does not change for fibers in the grid orientation. Then, the total penetration is the ratio of particles initially positioned further than $\eta_C(D_f+D_p)/2$ from a fiber center, $\rho_p\left(h + D_f - \eta_C\left(D_f + D_p\right)\right)^2$, to the total number of particles approaching the filter, $\rho_p\left(h + D_f\right)^2$, where ρ_p is the number of particles per cross sectional area of the grid. We assume particles approaching the grid have uniformly distributed initial positions such that the penetration is given by,

$$P_{coul}^{sim} = \frac{C_{V>0}}{C_{V=0}} = \frac{\left(h+D_f-\eta_C\left(D_f+D_p\right)\right)^2}{\left(h+D_f\right)^2} \tag{2}$$

This simulated columbic penetration can be directly compared to that obtained from experiments. The COMSOL Multiphysics software was used to solve the Poisson and Navier-Stokes equations as well as to integrate the equations of motion for particle trajectories. All parameters used in the simulation are listed in Table 1.

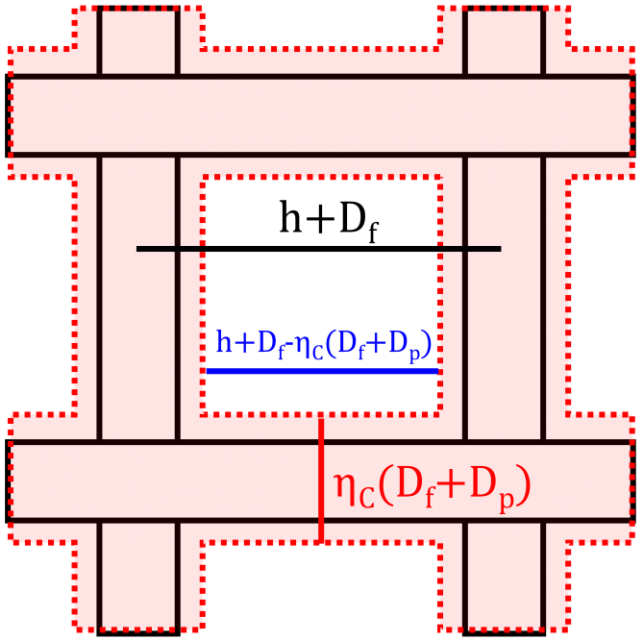

Figure 4. Schematic of the grid arrangement of fibers used to calculate the total penetration through a metallic grid from the single fiber efficiency, η_C, calculated from the trajectory simulations. Particles with initial positions within the shaded red region are captured by the fiber.

Table 1. Parameters used in particle trajectory simulations. All of these parameters have a direct basis from the experimental system. Other relevant parameters not listed include the viscosity, density and permittivity of air.

Parameter	Symbol	Value/Range
Particle diameter	D_p	70 - 500 nm
Particle charge	q	$1e^-$
Fiber diameter	D_f	100 μm
Fiber spacing	h	250 μm
Grid spacing	d	11 mm
Applied potential difference	ΔV	0 - 6000 V
Airflow face velocity	u	0.6 - 5 cm/s

III. RESULTS AND DISCUSSION

Figure 5 shows the experimental results for P_{coul} through the filter assembly as a function of the applied potential difference between the high-voltage grid and grounded grids, the airflow velocity at the face of the grid, and the particle diameter. We note that in all data presented, aerosol particles have one negative elementary charge, the middle metallic grid has a positive applied potential, and the metallic grid has fiber diameter of 100 μm and spacing of 250 μm. We emphasize that all parameters used in our simulation have values taken from our experimental system i.e. *no fitting parameters are used*.

As shown in Figure 5a, P_{coul} decreases as the applied potential difference increases. This effect occurs because the attractive forces between the particles and fibers increase with greater applied potential differences.

As shown in Figure 5b, P_{coul} increases as the airflow velocity increases. With higher airflow velocity, the particles spend less time in proximity of the high-voltage grid. Thus, electrostatic forces do not displace particles as significantly toward the fibers and the penetration increases.

As shown in Figure 5c, P_{coul} increases as the particle diameter increases. As the particle diameter increases, the drag force on the particle increases, which decreases the drift velocity of the particles towards the fiber. Meanwhile the coulombic attractive force between the particles and fibers remain the same since the particle charge is constant.

The coulombic penetration predicted from simulations agrees with experiments very well at large particle sizes but overestimates the penetration as the particles size decreases. Our analysis below suggests a reason for this overestimation at small particle sizes.

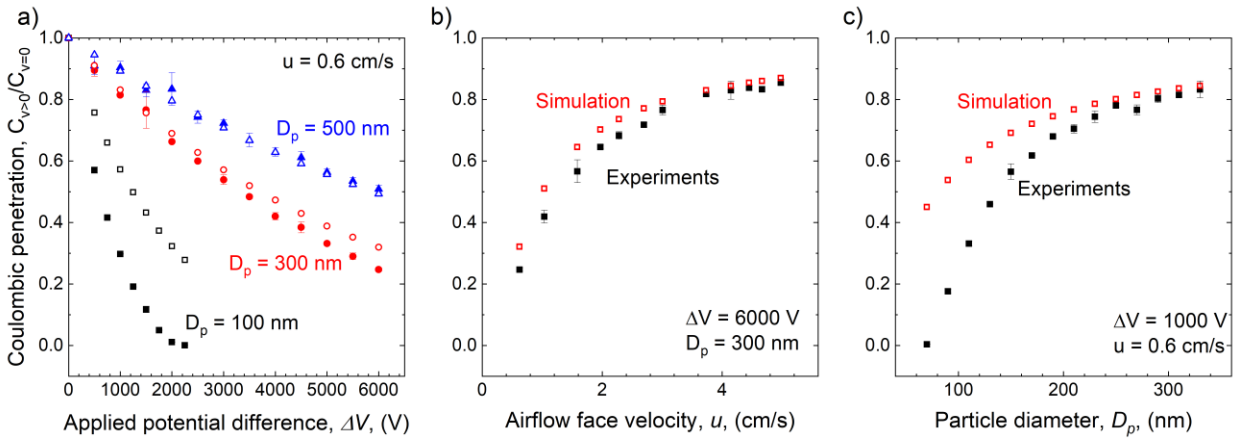

Figure 5. Coulombic penetration as a function of a) applied potential difference at a constant u = 0.6 cm/s at three particle diameters: D_p = 100 nm (black), D_p = 300 nm (red), D_p = 500 nm (blue); b) airflow face velocity at a constant D_p = 300 nm and ΔV = 1000 V; c) particle diameter at a constant u = 0.6 cm/s and ΔV = 1000 V. Open points are data from particle trajectory simulations and solid points are from experiments. In c) aerosol particles are generated from a potassium chloride (KCl) solution and monodisperse, singly charged KCl particles are sorted using the DMA.

Our simulation methodology employs some simplifying assumptions to model the experimental system. In particular, we do not account for nonuniform airflow velocities. Indeed, the average airflow face velocities examined ranged between 0.6 – 5 cm/s and in our analysis was considered to be uniform over the face of the grids. Thus, we do not account for nonuniform inlet fluid velocities which may arise in experiments due to undeveloped flow profiles or edge effects at the perimeter of the filter holder. This is justified by that fact that, due to the small Reynolds number (fluid velocities tested <5 cm/s), the regime is laminar with low inertial effects, thus we do not expect these effects to be significant. Instead, we hypothesize that the discrepancy between experiments and simulation at small particle sizes is a result of molecular slip which is more significant for small particles and is not accounted for in the simulation.

To characterize the significance of molecular slip in our system, we examine the single fiber efficiency since it is a more general quantity that is normalized with respect to the filter thickness. We estimate the experimental coulombic single fiber efficiency by rearranging Eq. 2. In Fig. 6, we compare the experimental and simulated single fiber efficiencies for all of the data shown in Fig. 5. In this Figure, we distinguish conditions where the Knudsen number is “high” and “low” by grouping conditions where the Knudsen number is greater than or less than 1 respectively. The Knudsen number,

$$Kn = 2\lambda/D_p \qquad (3)$$

where λ, is the molecular mean free path of air (~65 nm), relates the degree to which fluid flow around aerosol particles can be treated as a continuum flow. At larger Knudsen numbers where the particle size is smaller than or on the same order as λ, the continuum flow assumption breaks down as air molecules "slip" past the aerosol particles, decreasing the fluid drag. The experiments and simulation agree more closely at small Knudsen numbers, where flow around particles is better approximated by continuum flow, and Stokes law applies for calculation of the drag force. At larger Knudsen numbers, the simulation, which does not account for molecular slip, overestimates drag forces on aerosol particles causing the drift velocity of particles toward fibers, and consequently the filtration efficiency, to be underestimated in the simulation.

We develop a dimensionless coulomb number, K_C, which is the ratio of the drift velocity due to coulomb attraction to the airflow velocity. The drift velocity, v_d, is obtained by setting the coulombic force equal to the Stokes drag force $3\pi\mu D_p v_d/C$ (μ is the viscosity of air) and solving for v_d. To account for molecular slip, we include the Cunningham slip correction factor, C. The coulomb force on a particle *far from the fibers* and between the high-voltage and grounded grids, is $q\Delta V/d$ (q is the charge on each aerosol particle); since the electric field nearby the fiber is enhanced at smaller D_f and larger h, we scale the characteristic coulomb force accordingly: $q\Delta Vh/dD_f$. Therefore, we obtain the coulomb number as:

$$K_C = \frac{q\Delta VhC}{3\pi\mu D_p d D_f u} \tag{4}$$

Physically, small values of K_C signify that particle drift due to electrostatic forces is small relative to fluid velocities causing electrostatic forces to have little effect on the efficiency. Large values of K_C indicate that attractive electrostatic forces dictate the trajectories of particles as opposed to fluid drag causing efficiency to be significantly enhanced due to attractive electrostatic effects. A similar coulomb number has previously been developed for the case of a fiber with constant charge density, rather than the present case of a fiber with constant electrostatic potential (Natanson, 1957).

Figure 7 depicts the experimental and simulated coulombic single fiber efficiencies as a function of the dimensionless coulomb number described from Eq. 4. Since molecular slip is not accounted for in the simulation, we consider K_C with $C = 1$ for the simulated results (Fig. 7b). On the other hand, since molecular slip affects the experimental results, we account for slip in K_C in the experiments (Fig. 7a) using the Cunningham correction,

$$C = 1 + Kn(\alpha + \beta \exp\left(-\frac{\gamma}{Kn}\right) \tag{5}$$

Where α, β, and γ are 1.257, 0.4, and 1.1 respectively, as is commonly used for spheres in air (C N Davies, 1945). For both experimental and simulation results, we fit η_C to K_C using a power-law expression. We find that in both the experiments and simulation, η_C scales very well with K_C as indicated by the R^2 values close to 1. Furthermore, we find excellent agreement in the scaling of η_C with K_C between the experiments and simulation (power-law exponents of 0.914 and 0.911 respectively) and very good agreement in the magnitude coefficient as well (12.7 and 16.1 respectively).

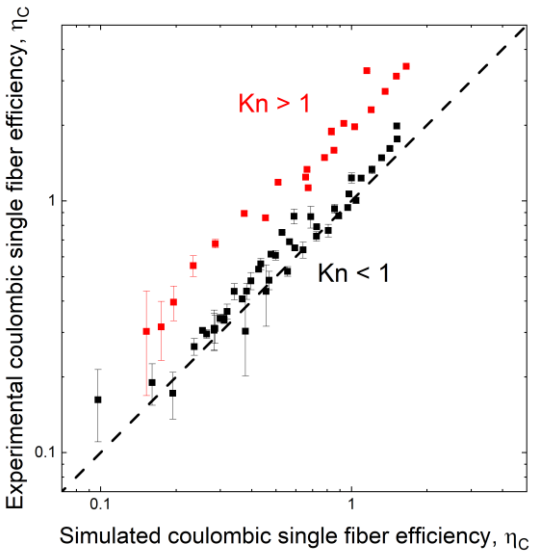

Figure 6. Simulated coulombic single fiber efficiency vs the experimental coulombic single fiber efficiency. The black dashed line represents where the simulation and experimental results are equal. Black data points have conditions where the Knudsen number is less than 1 and red data points have conditions where the Knudsen number is greater than 1.

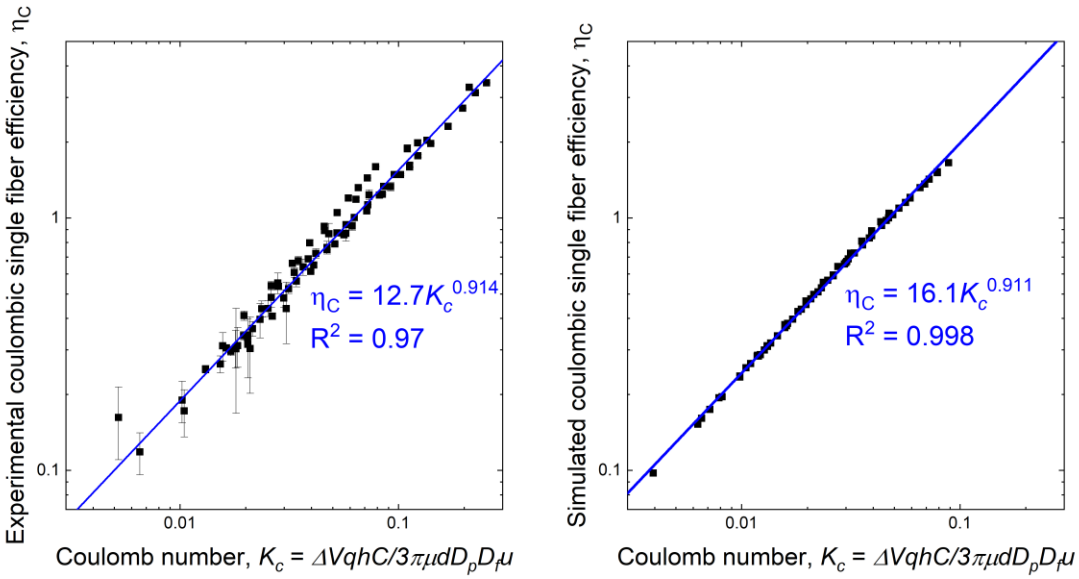

Figure 7. The a) experimental and b) simulated coulombic single fiber efficiency as a function of the coulomb number. In a) C in K_C is calculated using Eq. 5 whereas in b) $C = 1$.

The effect of electrostatic interactions on aerosol filtration performance has long been the subject of study, but rigorous experimental control over electrostatic interactions has been elusive due to difficulty controlling the charge and potential distribution in filter media. More recently, progress has been made in controlling electrostatic properties of filter media, both for the purpose of fundamental investigation of electrostatic filtration effects (Alonso et al., 2007), and for application in active-electrostatically assisted filtration (Choi et al., 2018, 2017; K. S. Han et al., 2019; S. Han et al., 2021; Jeong et al., 2017; Tian & Mo, 2019; Tian et al., 2021; G. H. Zhang et al., 2020; R. Y. Zhang & Hsieh, 2020; K. Zhao et al., 2020).

Alonso et al. probed the role of electrostatic image forces (where charged particles polarize fibers creating an attractive force) in filtration of nano-scale charged aerosols by using grounded metallic grids as the filter media (Alonso et al., 2007). This filter media was advantageous since the image force between a charged particle and a grounded wire is well-defined and the uniform size, spacing, and orientation of wires in the metallic grid facilitated consistent image forces throughout the filter media. Similarly, coulomb forces have previously been controlled to a certain extent by applying potentials to complex, nonuniform conductive filter media, yet the complexity of these systems precluded rigorous evaluation these electrostatic interactions.

The filter assembly developed here integrates ideas from these prior works to precisely control coulombic forces—we apply a potential to the filter media and ensure the potential distribution is uniform and well-defined by using a metallic grid with adjacent electrically grounded grids on either side of the high-voltage grid. Our experiments clearly demonstrate that coulombic forces substantially enhance filtration efficiency particularly within the typical MPPS regimes tested in this study.

The simulations of this well-controlled experimental system elucidate key physics governing particle capture within the filter. In particular, the comparison between experiments and simulation at small particle sizes indicate the importance of non-continuum, “slip” effects at high Knudsen numbers. This slip, weakens drag forces on aerosol particles, thereby increasing displacement of particles toward fibers due to coulombic forces and consequently improves the filter efficiency. Prior works have developed corrections to the drag forces at high Knudsen numbers in effort to address these slip effects (Allen & Raabe, 1985; C N Davies, 1945; Cunningham, 1910; Millikan, 1910).

Both experiments and simulations scale well with the coulomb number developed here which is applicable to the constant electrical potential limit of charged fibers (in contrast to the constant charge limit developed in prior work (Kraemer & Johnstone, 1956; Natanson, 1957; Zebel, 1965)). Further, we emphasize that this coulomb number is developed for the case where each charged fiber is adjacent to equally spaced electrical grounds, and thus may not be applicable to more general, complex conductive filter media used in prior studies (Choi et al., 2018, 2017).

Though electrostatic interactions between particles and fibers are well-known to increase the efficiency of a clean filter, many open questions still remain regarding, in particular, how electrostatic interactions impact the long-term performance of a filter. As filters are used, particles accumulate on the fibers of the filter changing both the fluid flow, as well as the electric field

distribution around the fibers. Electrostatic interactions change the particle deposit distributions around fibers and prior work along with the present trajectory simulations suggest that electrostatic interactions cause particles to deposit more uniformly on the upstream and downstream sides of fibers (Kanaoka, Hiragi, & Tanthapanichakoon, 2001; D. C. Walsh & Stenhouse, 1997a, 1997b, 1998; D. Walsh & Stenhouse, 1996).

However, complexity of real filter media makes systematic investigation of how electrostatic effects change the loading of filters challenging. Furthermore, analytically determining the trajectories of particles around fibers, as has previously been done for clean fibers (Kraemer & Johnstone, 1956; Natanson, 1957; Zebel, 1965), is not possible for fibers loaded with particles. As such, experimental methodologies with more highly controlled filter properties and more robust modeling methods are required for a fundamental understanding of how electrostatic interactions affect the long-term performance of filters.

To the authors' knowledge, the experimental methodology in the present work is the first to control all aspects of the filter media and aerosol as to achieve excellent quantitative agreement in the electrostatic filtration efficiency with particle trajectory simulations without any fitting parameters. Experiments with this filter assembly can be adjusted to systematically test complexities in real electret filter media. For instance, inter-fiber spacing can be varied by using a finer grid to investigate the role of fiber proximity on electrostatic capture, or clogging studies may elucidate how previously deposited particles affect further electrostatic capture. As such, the experimental and simulation methodologies developed here provide valuable tools to address remaining open questions in electrostatic filtration from a fundamental, rather than empirical, perspective.

IV. CONCLUSION

We develop an aerosol filtration bench wherein electrical and geometrical properties of both aerosol particles and the filter media are precisely controlled. Using this filtration bench we demonstrate that coulombic interactions significantly enhance filtration efficiency and can be tuned in our filter assembly by varying the applied voltage. We develop particle trajectory simulations designed to model our experimental system and find excellent quantitative agreement between simulations and experiments *without any fitting parameters*. The combination of the experimental and simulation methodologies developed here elucidate key fundamental physics governing electrostatic filtration and are valuable to examine more complicated phenomena in electret filters such as clogging.

References

Allen, M. D., & Raabe, O. G. (1985). Slip Correction Measurements of Spherical Solid Aerosol Particles in an Improved Millikan Apparatus. *Aerosol Science and Technology*, *4*(3), 269–286. https://doi.org/10.1080/02786828508959055

Alonso, M., Alguacil, F. J., Santos, J. P., Jidenko, N., & Borra, J. P. (2007). Deposition of ultrafine aerosol particles on wire screens by simultaneous diffusion and image force. *Journal of Aerosol Science*, *38*(12), 1230–1239. https://doi.org/10.1016/j.jaerosci.2007.09.004

Anderson, E. L., Turnham, P., Griffin, J. R., & Clarke, C. C. (2020). Consideration of the Aerosol Transmission for COVID-19 and Public Health. *Risk Analysis*, *40*(5), 902–907. https://doi.org/10.1111/risa.13500

Baumgartner, H., & Loffler, F. (1986). The collection performance of electret filters in the particle size range 10 nm - 10 um. *Journal of Aerosol Science*, *17*(3), 438–445.

C N Davies. (1945). Definitive equations for the fluid resistance of spheres. *Proceedings of the Physical Society*, *57*(4), 259–270. https://doi.org/10.1088/0959-5309/57/4/301

Choi, D. Y., An, E. J., Jung, S. H., Song, D. K., Oh, Y. S., Lee, H. W., & Lee, H. M. (2018). Al-Coated Conductive Fiber Filters for High-Efficiency Electrostatic Filtration: Effects of Electrical and Fiber Structural Properties. *Scientific Reports*, *8*(1), 1–10. https://doi.org/10.1038/s41598-018-23960-9

Choi, D. Y., Jung, S.-H., Song, D. K., An, E. J., Park, D., Kim, T., … Lee, H. M. (2017). Al-Coated Conductive Fibrous Filter with Low Pressure Drop for Efficient Electrostatic Capture of Ultrafine Particulate Pollutants. *ACS Applied Materials & Interfaces*, *9*(19), 16495–16504. https://doi.org/10.1021/acsami.7b03047

Cowling, B. J., Ip, D. K. M., Fang, V. J., Suntarattiwong, P., Olsen, S. J., Levy, J., … Mark Simmerman, J. (2013). Aerosol transmission is an important mode of influenza A virus spread. *Nature Communications*, *4*. https://doi.org/10.1038/ncomms2922

Cunningham, E. (1910). On the velocity of steady fall of spherical particles through fluid medium. *Proceedings of the Royal Society of London. Series A, Containing Papers of a Mathematical and Physical Character*, *83*(563), 357–365. https://doi.org/10.1098/rspa.1910.0024

Halverson, M., Ballinger, M., & Dennis, G. (1987). *Combustion aerosols formed during burning of radioactively contaminated materials: Experimental results*. *Report*. Richland, WA (United States). https://doi.org/10.2172/6900062

Han, K. S., Lee, S., Kim, M., Park, P., Lee, M. H., & Nah, J. (2019). Electrically Activated Ultrathin PVDF-TrFE Air Filter for High-Efficiency PM1.0 Filtration. *Advanced Functional Materials*, *29*(37), 1–7. https://doi.org/10.1002/adfm.201903633

Han, S., Kim, J., & Ko, S. H. (2021). Advances in air filtration technologies: structure-based and interaction-based approaches. *Materials Today Advances*, *9*. https://doi.org/10.1016/j.mtadv.2021.100134

Jeong, S., Cho, H., Han, S., Won, P., Lee, H., Hong, S., … Ko, S. H. (2017). High Efficiency, Transparent, Reusable, and Active PM2.5 Filters by Hierarchical Ag Nanowire Percolation Network. *Nano Letters*, *17*(7), 4339–4346. https://doi.org/10.1021/acs.nanolett.7b01404

Kanaoka, C., Hiragi, S., & Tanthapanichakoon, W. (2001). Stochastic simulation of the agglomerative deposition process of aerosol particles on an electret fiber. *Powder Technology*, *118*(1–2), 97–106. https://doi.org/10.1016/S0032-5910(01)00299-6

Kaneyasu, N., Ohashi, H., Suzuki, F., Okuda, T., & Ikemori, F. (2012). Sulfate aerosol as a potential transport medium of radiocesium from the fukushima nuclear accident. *Environmental Science and Technology*, *46*(11), 5720–5726. https://doi.org/10.1021/es204667h

Kerner, M., Schmidt, K., Hellmann, A., Schumacher, S., Pitz, M., Asbach, C., … Antonyuk, S. (2018). Numerical and experimental study of submicron aerosol deposition in electret microfiber nonwovens. *Journal of Aerosol Science*, *122*(May), 32–44. https://doi.org/10.1016/j.jaerosci.2018.05.004

Kerner, M., Schmidt, K., Schumacher, S., Puderbach, V., Asbach, C., & Antonyuk, S. (2020). Evaluation of electrostatic properties of electret fi lters for aerosol deposition. *Separation and Purification Technology*, *239*(November 2019), 116548. https://doi.org/10.1016/j.seppur.2020.116548

Kilic, A., Shim, E., & Pourdeyhimi, B. (2015). Measuring electrostatic properties of fi brous materials : A review and a modi fi ed surface potential decay technique. *Journal of Electrostatics*, *74*, 21–26. https://doi.org/10.1016/j.elstat.2014.12.007

Kim, J. C., Otani, Y., Noto, D., Namiki, N., & Kimura, K. (2005). Initial Collection Performance of Resin Wool Filters and Estimation of Charge Density. *Aerosol Science and Technology*, *39*(6), 501–508. https://doi.org/10.1080/027868291001394

Kraemer, H. F., & Johnstone, H. F. (1956). Collection of Aerosol Particles in Presence of Electrostatic Fields. *Industrial & Engineering Chemistry*, *48*(4), 812–812. https://doi.org/10.1021/ie50556a042

Lathrache, R., & Fissan, H. (1986). Fractional Penetrations for Electrostatically Charged Fibrous Filters in the Submicron Particle Size Range. *Particle & Particle Systems Characterization*, *3*(2), 74–80. https://doi.org/10.1002/ppsc.19860030206

Lathrachi, R., Fissan, H., & Neuman, S. (1986). Deposition of submicron particles on electrically charged fibers. *Journal of Aerosol Science*, *17*(3), 446–449.

Lee, M., Otani, Y., Namiki, N., & Emi, H. (2002). Prediction of collecion efficiency of high-perfromance electret filters. *Journal of Chemical Engineering of Japan*, *35*(1), 57–62.

Malá, H., Rulík, P., Bečková, V., Mihalík, J., & Slezáková, M. (2013). Particle size distribution of radioactive aerosols after the Fukushima and the Chernobyl accidents. *Journal of Environmental Radioactivity*, *126*, 92–98. https://doi.org/10.1016/j.jenvrad.2013.07.016

Millikan, R. A. (1910). The Isolation of an Ion, a Precision Measurement of Its Charge, and the Correction of Stokes's Law. *Science*, *32*(822), 436–448. https://doi.org/10.1126/science.32.822.436

Natanson, G. L. (1957). Deposition of aerosol particles by electrostatic attraction upon a cylinder around which they are flowing. *Dokl Akad Nauk USSR*, *112*, 696–699.

Povinec, P. P., Sýkora, I., Holý, K., Gera, M., Kováčik, A., & Brest'áková, L. (2012). Aerosol radioactivity record in Bratislava/Slovakia following the Fukushima accident - A comparison with global fallout and the Chernobyl accident. *Journal of Environmental Radioactivity*, *114*, 81–88. https://doi.org/10.1016/j.jenvrad.2012.05.008

Romay, F. J., Liu, B. Y. H., & Chae, S. (1998). Experimental Study of Electrostatic Capture Mechanisms in Commercial Electret Filters. *Aerosol Science and Technology*, *28*(3), 224–234. https://doi.org/10.1080/02786829808965523

Sow, M., Leblois, Y., Bodiot, C., Motzkus, C., Ritoux, S., & Gensdarmes, F. (2020). Aerosol release fraction by concrete scarifying operations and its implications on the dismantling of nuclear facilities. *Journal of Hazardous Materials*, *400*(March), 123077. https://doi.org/10.1016/j.jhazmat.2020.123077

Sow, M., Leblois, Y., & Gensdarmes, F. (2019). Experimental study of aerosol release following liquid leaks of fission products concentrates simulants. *Nuclear Engineering and Design*, *341*(September 2018), 46–55. https://doi.org/10.1016/j.nucengdes.2018.09.034

Thakur, R., Das, D., & Das, A. (2013). Electret Air Filters. *Separation & Purification Reviews*, *42*(2), 87–129. https://doi.org/10.1080/15422119.2012.681094

Thakur, R., Das, D., Das, A., & Reddy, C. C. (2015). Spatial charge distribution in fi brous dielectrics. *Journal of Electrostatics*, *76*, 1–7. https://doi.org/10.1016/j.elstat.2015.03.010

Thomas, D., Mouret, G., Cadavid-Rodriguez, M. C., Chazelet, S., & Bémer, D. (2013). An improved model for the penetration of charged and neutral aerosols in the 4 to 80nm range through stainless steel and dielectric meshes. *Journal of Aerosol Science*, *57*, 32–44. https://doi.org/10.1016/j.jaerosci.2012.10.007

Tian, E., & Mo, J. (2019). Toward energy saving and high efficiency through an optimized use of a PET coarse filter: The development of a new electrostatically assisted air filter. *Energy and Buildings*, *186*, 276–283. https://doi.org/10.1016/j.enbuild.2019.01.021

Tian, E., Yu, Q., Gao, Y., Wang, H., Wang, C., Zhang, Y., … Li, J. (2021). Ultralow Resistance Two-Stage Electrostatically Assisted Air Filtration by Polydopamine Coated PET Coarse Filter. *Small*, *17*(33), 1–13. https://doi.org/10.1002/smll.202102051

Vohra, K., Vodonos, A., Schwartz, J., Marais, E. A., Sulprizio, M. P., & Mickley, L. J. (2021). Global mortality from outdoor fine particle pollution generated by fossil fuel combustion : Results from GEOS-Chem. *Environmental Research*, *195*(February), 110754. https://doi.org/10.1016/j.envres.2021.110754

Walsh, D. C., & Stenhouse, J. I. T. (1997a). Clogging of an electrically active fibrous filter material : experimental results and two-dimensional simulations, *93*, 63–75.

Walsh, D. C., & Stenhouse, J. I. T. (1997b). The effect of particle size, charge, and composition on the loading characteristics of an electrically active fibrous filter material. *Journal of Aerosol Science*, *28*(2), 307–321.

Walsh, D. C., & Stenhouse, J. I. T. (1998). Parameters Affecting the Loading Behavior and Degradation of Electrically Active Filter Materials. *Aerosol Science and Technology*, *29*(5), 419–432. https://doi.org/10.1080/02786829808965580

Walsh, D., & Stenhouse, I. (1996). Experimental Studies of Electrically Active Fibrous Filter Loading. *Particle & Particle Systems Characterization*, *13*, 47–53.

Wu, Z., Colbeck, I., & Zhang, G. (1993). Deposition of Particles on a Single Cylinder by a Coulombic Force and Direct Interception. *Aerosol Science and Technology*, *19*(1), 40–50. https://doi.org/10.1080/02786829308959619

Zebel, G. (1965). Deposition of aersol flowing past a cylindrical fiber in a uniform electric field. *Journal of Colloid Science*, *543*, 522–543.

Zhang, G. H., Zhu, Q. H., Zhang, L., Yong, F., Zhang, Z., Wang, S. L., … Tao, G. H. (2020). High-performance particulate matter including nanoscale particle removal by a self-powered air filter. *Nature Communications*, *11*(1). https://doi.org/10.1038/s41467-020-15502-7

Zhang, R. Y., & Hsieh, G. W. (2020). Electrostatic polyester air filter composed of conductive nanowires and photocatalytic nanoparticles for particulate matter removal and formaldehyde decomposition. *Environmental Science: Nano*, *7*(12), 3746–3758. https://doi.org/10.1039/d0en00683a

Zhao, K., Huang, J., Mao, J., Bao, Z., Chen, Z., & Lai, Y. (2020). Charged graphene aerogel filter enabled superior particulate matter removal efficiency in harsh environment. *Chemical Engineering Journal*, *395*(February), 125086. https://doi.org/10.1016/j.cej.2020.125086

Zhao, M., Liao, L., Xiao, W., Yu, X., Wang, H., Wang, Q., … Cui, Y. (2020). Household Materials Selection for Homemade Cloth Face Coverings and Their Filtration Efficiency Enhancement with Triboelectric Charging. *Nano Letters*, *20*(7), 5544–5552. https://doi.org/10.1021/acs.nanolett.0c02211